

# Development of Novel Benzomorpholine Class of Diacylglycerol Acyltransferase I Inhibitors

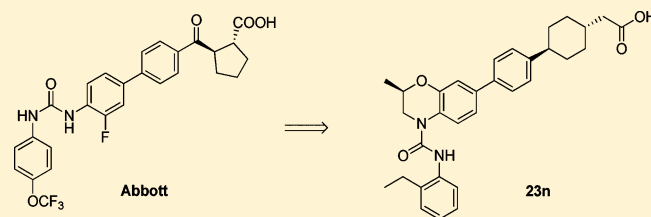
Gang Zhou,\* Nicolas Zorn, Pauline Ting, Robert Aslanian, Mingxiang Lin, John Cook, Jean Lachowicz, Albert Lin, Michelle Smith, Joyce Hwa, Margaret van Heek, and Scott Walker

Discovery and Preclinical Sciences, Merck Research Laboratories, 126 East Lincoln Avenue, Rahway, New Jersey 07065, United States

## Supporting Information

**ABSTRACT:** Diacylglycerol acyltransferase 1 (DGAT1) presents itself as a potential therapeutic target for obesity and diabetes for its important role in triglyceride biosynthesis. Herein we report the rational design of a novel class of DGAT1 inhibitors featuring a benzomorpholine core (**23n**). SAR exploration yielded compounds with good potency and selectivity as well as reasonable physical and pharmacokinetic properties. This class of DGAT1 inhibitors was tested in rodent models to evaluate DGAT1 inhibition as a novel approach for the treatment of metabolic diseases. Compound **23n** conferred weight loss and a reduction in liver triglycerides when dosed chronically in mice with diet-induced obesity and depleted serum triglycerides following a lipid challenge.

**KEYWORDS:** DGAT1, diacylglycerol acyltransferase inhibitor, benzomorpholine, postprandial triglyceridemia (PPTG)



Disorders in triglyceride (TG) metabolism (dyslipidemia) related to either absorption or *de novo* synthesis have been implicated in the pathogenesis of a variety of diseases and risk factors, including obesity, type II diabetes, dyslipidemia, metabolic syndrome, atherosclerosis, and coronary heart disease.<sup>1,2</sup> Therapeutic agents that can decrease the synthesis of TG by inhibiting enzymes in corresponding metabolic pathways may be valuable as therapeutic options for the treatment of dyslipidemia.<sup>3</sup>

Acyl-CoA:diacylglycerol acyltransferase (DGAT), which is widely expressed in mammalian adipose tissue, small intestine, liver, and mammary gland, is a potential therapeutic target because it catalyzes the final step of esterification of 1,2-diacylglycerol with fatty acyl CoA to form triglycerides at the endoplasmic reticulum.<sup>4,5</sup> In theory, DGAT plays an essential role in the metabolism of cellular diacylglycerol and is critically important for triglyceride absorption and production as well as energy storage homeostasis.<sup>6</sup> Two DGAT enzymes DGAT1 and DGAT2, which are encoded by a distinct gene family, share very limited sequence homology.<sup>7,8</sup> Research has shown that knockout DGAT1 mice (DGAT1<sup>-/-</sup>) are resistant to diet-induced obesity,<sup>9</sup> exhibit increased insulin sensitivity relative to wild-type littermates,<sup>10</sup> and have decreased adiposity (probably due to increased energy expenditure).<sup>11</sup> On the contrary, DGAT2<sup>-/-</sup> mice are not viable due to lipopenia and skin homeostasis abnormalities.<sup>12</sup> The large body of genetic, biochemical, and phenotypic evidence has spurred intense research efforts to discover selective, small molecule inhibitors of DGAT1.<sup>13–19</sup> Typical representative structures are shown in Figure 1.<sup>14–19</sup> While structural diversity is noticeable among the reported DGAT1 inhibitors, most possess a carboxylic acid moiety. Several candidates display excellent dose-dependent

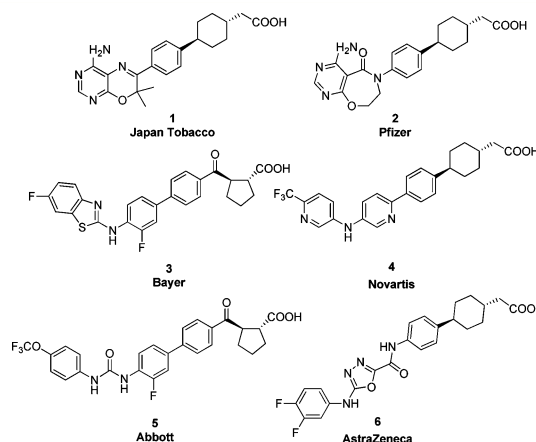


Figure 1. Structures of selected DGAT1 inhibitors.

weight gain inhibition in diet induced obesity (DIO) models and have entered clinical trials.<sup>16</sup>

The structural analysis of these compounds inspired us to use compound **5**<sup>18</sup> (green) as the starting point for pharmacophore modeling. Key elements of the pharmacophore-based modeling approach of our efforts are presented in Figure 2. Indole compound **7** (yellow) was initially proposed to probe the effects of torsional constraints on the urea motif by formation of an additional ring. This modification appeared structurally to be well tolerated because overlap of the urea hydrogen bond

Received: December 22, 2013

Accepted: March 1, 2014

Published: March 1, 2014

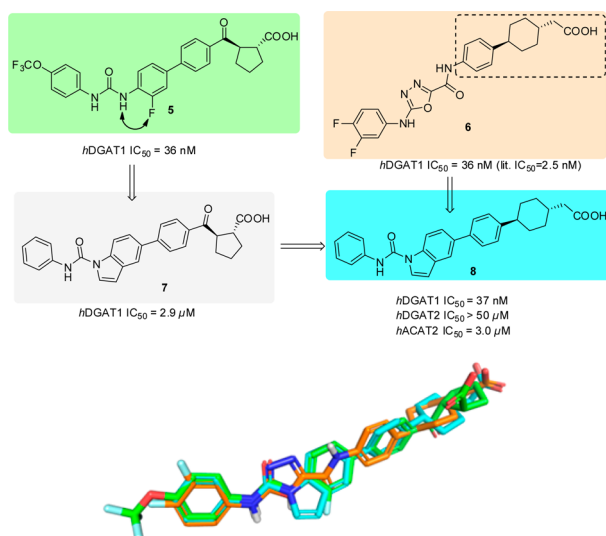


**Figure 2.** Lead structure design based on Abbott and AstraZeneca DGAT1 inhibitors. Pharmacophore models of 5 (green), 6 (yellow), and 8 (cyan) were developed with full conformational analysis for the lowest energy conformations (Sybyl 8.0).

donor and acceptor features was observed between compounds 5 and 7. To our surprise, *in vitro* DGAT1 data for indole 7 showed low enzyme inhibition. Further modeling work suggested it is beneficial to replace the benzoylcyclopentyl carboxylic acid fragment of compound 7 with the phenylcyclohexaneacetic acid moiety, as presented in many reported DGAT1 inhibitors, including compound 6.<sup>14</sup> Model overlay of the resulting indole inhibitor 8 with AstraZeneca amino-oxadiazole 6 showed excellent alignment of all pharmacophore features. This proposal was later confirmed by a dramatic improvement in DGAT1 enzyme potency for indole 8 over 7.

Lead compound 8 displayed encouraging properties. It showed selectivity for DGAT1 over DGAT2 and ACAT enzymes ( $\sim 100$ -fold), acceptable physicochemical and pharmacokinetic properties (MW = 455, Caco2 = 170 nm/s, sol = 20  $\mu\text{M}$ , PPB = 99.8%, *in vitro*  $\text{Cl}_{\text{rat/hu}}$  = 3.9/7.6  $\mu\text{L}/\text{min}/\text{Mcells}$ , reasonable rat oral bioavailability and half-life) and presented no off-target liability except CYP 1A1 induction (3-fold at 30  $\mu\text{M}$ ). When dosed orally in mice, compound 8 demonstrated moderate efficacy measured by triacylglyceride reduction in our *in vivo* postprandial triglyceridemia (PPTG) assay ( $-45\%$  at 10 mg/kg @ 2 h). However, instability issues were revealed when decomposition of indole 8 in both human and mouse plasma was observed ( $\sim 40\%$  loss of parent compound measured in *in vitro* human plasma at 25  $^{\circ}\text{C}$  after 12 h). Furthermore, the decomposition of 8 generated a potentially genotoxic aniline byproduct under these conditions. Therefore, our lead optimization strategy was focused on improving both *in vitro* and *in vivo* DGAT1 potency while increasing plasma stability.

We reasoned that the plasma stability issue of 8 is probably due to the indole urea moiety. Further research was focused on scaffold replacements of the indole ring and rapidly identified benzomorpholine compound 9 with improved plasma stability *in vitro* activity and *in vivo* efficacy. Triglyceride levels in the PPTG assay were decreased by 52% at 10 mg/kg in comparison to the vehicle. Pharmacokinetic properties for compounds 9 were dramatically improved (AUC = 58  $\mu\text{M}\cdot\text{h}$  at 10 mg/kg,  $t_{1/2}$  = 4 h, rat oral bioavailability  $>90\%$ ) due to the combination of improved solubility (100  $\mu\text{M}$ ), Caco2 permeability (448 nm/s),

low clearance ( $\text{Cl}_{\text{rat/hu}}$  = 9/11  $\mu\text{L}/\text{min}/\text{Mcells}$ ), and better plasma stability ( $\sim 10\%$  loss of parent compound measured in human plasma at 25  $^{\circ}\text{C}$  after 12 h). Compound 9 also demonstrated acceptable selectivity over *h*DGAT2 ( $\text{IC}_{50}$   $>10$   $\mu\text{M}$ ), *h*ACAT2 ( $\text{IC}_{50}$  = 9.7  $\mu\text{M}$ ), and a clean ancillary profile except CYP 1A1 induction (10-fold at 30  $\mu\text{M}$ ). As a result, the benzomorpholine class emerged as the new lead series for optimization.

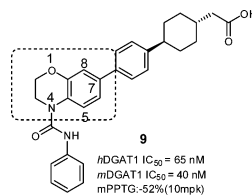
The results of subsequent SAR investigations of the benzomorpholine core are summarized in Table 1. Changing the topology by moving the *trans*-phenylcyclohexaneacetic acid substituent around the benzomorpholine ring resulted in dramatic potency loss (to C-8 and C-6 positions in compounds 10 and 11, respectively). Incorporation of nitrogen into the core aromatic ring was not tolerated (analog 12 and 13). Introduction of a methyl group at the oxazine C-3 position (compounds 14) proved to be detrimental to activity. In contrast, introduction of a methyl group at the oxazine C-2 position (compound 16) increased *in vivo* efficacy (85% decrease of TG levels in PPTG assay compared to 9) as well as ACAT2 selectivity (*h*ACAT2  $\text{IC}_{50}$  = 5.0  $\mu\text{M}$ ) and plasma exposure levels. Addition of a carbonyl group at the C3-position of 16 resulted in an inactive compound (compound 15).

The SAR of the absolute stereochemistry in 16 was also investigated. (*S*)-Enantiomer 18 displayed 6-fold less activity relative to the *R*-enantiomer 17. (*R*)-Enantiomer 17 also demonstrated excellent triglyceride lowering effect *in vivo* as well as good selectivity over *h*DGAT2 and *h*ACAT1 ( $\text{IC}_{50}$  = 10  $\mu\text{M}$ ) and moderate selectivity over *h*ACAT2 ( $\text{IC}_{50}$  = 2.0  $\mu\text{M}$ ). Compound 17 had a clean off-target profile with the exception of moderate CYP450 2C9 liver enzyme inhibition ( $\text{IC}_{50}$  = 14  $\mu\text{M}$ ). It is not surprising that 2,2-dimethyl substitution at the C-2 position resulted in a 10-fold loss in potency (data not shown). One-carbon extension of the methyl group at the oxazine C-2 position was tolerated (as shown for compound 19), but further elongation of the alkyl chain (compound 20) or branching (analog 21) resulted in loss of potency.

In concert with the SAR exploration around the bicyclic core, extensive work was undertaken to optimize the urea moiety. Representative examples of these modifications are summarized in Table 2. Replacement of the urea motif in compounds 22a–d resulted in partial to complete loss of DGAT1 inhibition, showing the critical importance of the urea hydrogen bond acceptor–donor pattern. On the urea aromatic ring, small and lipophilic substituents were better tolerated at the *ortho*- and *para*-positions than at the *meta*-position, as shown in compounds 22e–j. Incorporation of polar substituents generally resulted in significant loss of activity (compounds 22k and 22l). This SAR trend was also observed in the indoline series (data not shown). Notably, fluorinated compound 22j displayed excellent *in vivo* efficacy (triacylglyceride reduction of 91% at 10 mg/kg and 59% at 3 mg/kg for the 2 h time-point compared to the vehicle-treated group), as well as good selectivity toward *h*DGAT2 (inactive), *h*ACAT1 ( $\text{IC}_{50}$  = 24  $\mu\text{M}$ ), and *h*ACAT2 ( $\text{IC}_{50}$  = 9.6  $\mu\text{M}$ ). Analog 22j also showed good PK properties (rat AUC = 23  $\mu\text{M}\cdot\text{h}$  @ 10 mg/kg, Caco2 = 239 nm/s, sol = 100  $\mu\text{M}$ , hepatocyte clearance of 19 and 1.0 mL/min/kg in human and rat, respectively) and *in vitro* safety profile (with no hERG, PXR, or liver enzymes inhibition or induction issues).

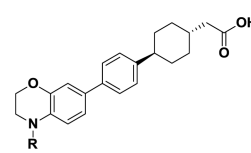
In an effort to alleviate issues related to the formation of potential genotoxic aniline metabolites, alkyl amines were also incorporated. In comparison to the aryl urea compound 9, the

Table 1. Core Modification on the Benzooxazine Ring



#	R	Human DGAT1 IC <sub>50</sub> (nM)	Mouse DGAT1 IC <sub>50</sub> (nM)	mPPTG %redn. of TG at 2 h (dose) AUC (10mg/kg)
10		>10000	>10000	NT
11		>10000	>10000	NT
12		>10000	>10000	NT
13		1900	550	NT
14		3100	630	NT
15		>10000	>10000	NT
16		91	33	-85% (10 mg/kg) 79 μM.h
17		43	18	-74% (3 mg/kg) 34 μM.h
18		530	360	NT
19		110	45	-88% (10 mg/kg) 63 μM.h
20		450	160	NT
21		560	300	NT

extended phenyl methyl urea analog **22m** suffered a 10-fold loss in DGAT1 activity. Further extension of the alkyl chain (e.g. phenylbutyl urea analog **22n**) helped regain *in vitro* potency for DGAT1 but was accompanied by loss of both *in vivo* biological activity (-23% TG reduction at 10 mg/kg) and selectivity over ACATs (~10× selectivity only). Short and branched aliphatic

Table 2. SAR Exploration of the Urea Moiety on the Dihydrobenzooxazine<sup>a,b</sup>


#	R	DGAT1 IC <sub>50</sub> (nM)	#	R	DGAT1 IC <sub>50</sub> (nM)
22a		580 (h) 110 (m)	22b		3700 (h)
22c		>10000	22d		>10000
22e		1700 (h) 1200 (m)	22f		69 (h) 34 (m)
22g		33 (h) 37 (m)	22h		20 (h) 16 (m)
22i		140 (h) 69 (m)	22j		20 (h) 35 (m)
22k		>10000	22l		6100 (h) 5200 (m)
22m		580 (h) 110 (m)	22n		91 (h) 36 (m)
22o		230 (h) 160 (m)	22p		32 (h) 27 (m)

<sup>a</sup>Assay values are the average of at least two independent determinations. <sup>b</sup>Enzyme species indicated between parentheses: h = human, m = mouse.

ureas generally suffered reduced *in vitro* DGAT1 potency (compound **22o**) while long aliphatic chains such as the heptanyleurea analog **22p** could restore *in vitro* potency levels of aryl ureas, while maintaining acceptable selectivity over DGAT2, ACAT1 (>100×), and ACAT2 (>20×) and a good safety profile. Compound **22p** is also particularly noteworthy because of its reasonable *in vivo* efficacy in the PPTG model (reduction of plasma TG levels by 48% at 3 mg/kg and 2 h time-point) in spite of its low plasma exposure after oral dosing, poor solubility, and low permeability (total rat AUC of 195 nM·h, C<sub>max</sub> of 65 nM at t<sub>max</sub> of 2 h with a plasma solubility at pH 7 of 5 μM and Caco2 of 35 nm/s). In a recent literature report,<sup>20</sup> experiments have shown that DGAT1 deficient mice with specific local expression of DGAT1 in the intestine completely reversed the resistance to diet induced obesity and hepatic steatosis normally associated with the DGAT1 knockout mouse, indicating that decreasing effects of DGAT1 on body weight are potentially attributed to the inhibition of the enzyme in the intestine. Compounds showing low systemic exposure,

such as **22p**, may be especially interesting because of the potentially reduced systemic toxicity.

Extensive work on the right-hand side carboxylic acid-containing fragment was also pursued to mitigate the potential risk of idiosyncratic toxicity associated with glucuronidation of the carboxylic acid moiety. Key examples selected from a large set of modifications are presented in Table 3. Initial implementation of common strategies involving increase of steric hindrance at the  $\alpha$ -position of the carboxylate or bioisosteric replacements led to loss of DGAT1 enzyme potency and *in vivo* efficacy (as exemplified by methyl-substituted analog **23a** or acid isosteres **23b–d**). Scaffold replacement efforts also showed limited success. Compound **23e**, bearing the *trans*-cyclopentane carboxylic acid piece reported by Abbott,<sup>18</sup> displayed a 10-fold loss of enzyme activity, a trend in agreement with the SAR observed in the indole series originally investigated. In addition, replacement of the *trans*-cyclohexaneacetic acid by its *cis* analog **23f** resulted in complete loss of *in vivo* efficacy in mice although good *in vitro* DGAT1 potency was retained. Alternatively, replacement of the cyclohexyl ring with some ether-linked acids (compounds **23g–j**) was explored in combination with a pyridyl moiety (to replace phenyl). Most of these compounds were less potent than the corresponding phenylcyclohexyl acid (compound **19**), except compound **23j**, which maintains potency. Surprisingly, **23j** compound was extremely efficacious *in vivo* with a 73% plasma TG level reduction at 0.3 mg/kg po dose in mice, along with excellent blood exposure (total rat AUC of 46  $\mu\text{M}\cdot\text{h}$  at 10 mg/kg) and clean off-target profile, except for inhibition of P450 2C9 liver enzyme ( $\text{IC}_{50} = 0.5 \mu\text{M}$ ) and induction of 2B liver enzyme (5-fold at 30  $\mu\text{M}$ ). The corresponding pyrimidine analogue (compound **23k**), however, is 5-fold less potent in enzyme activity.

Finally, the optimal groups in three regions (X, Y, and R as shown in structure **23**) were combined to provide compound **23l** and its enantiomers. Similarly, the (*R*)-enantiomer **23n** is more potent *in vivo* than the (*S*)-enantiomer **23m** even though they have similar *in vitro* potency. The reason for these discrepancies remains unclear.

Although several designed DGAT1 inhibitors were able to achieve very significant *in vivo* efficacy after a lipid challenge in our murine PPTG assay, we did not observe good correlation between pharmacodynamic (PPTG) and pharmacokinetic models within our acid series. To further explore other beneficial effects of this series of compounds, a body weight loss study was conducted to evaluate and benchmark chronic efficacy in a rodent model. Methyl-substituted benzooxazine **23n** was selected as a tool compound based on its good overall properties: long duration of plasma TG level reduction in mouse ( $-87\%$  at the 12 h time-point), high pH 7 solubility (50  $\mu\text{M}$ ), high Caco2 permeability (201 nm/s), acceptable hepatocyte clearance (14 and 10 mL/min/Mcells in human and rat, respectively), and clean ancillary profile (no P450 CYPs or P-gp inhibition, no PXR and CYP activation or ion channel activity, and no Ames toxicity).

Pharmacokinetic parameters for compound **23n** in key animal species are summarized in Table 4. Data collected in rats, mice, monkeys, and dogs confirmed the excellent oral bioavailability of **23n** and high protein binding (PPB > 99.5% in human and mouse), features also observed for other carboxylic acids within this chemotype.

The results of a chronic weight loss study in diet-induced obese mice are presented in Figure 3. During the 11-day

Table 3. Structure–Activity Relationship of Right-Hand Side Carboxylic Acid-Bearing Tails<sup>a,b</sup>

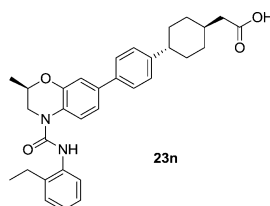
**23**

#	X	Y	R	DGAT1 IC <sub>50</sub> (nM)	mPPTG <sup>c</sup> %reduction of TG at 2 h (dose)
<b>23a</b>	H	H		950 (h) 200 (m)	NT
<b>23b</b>	H	H		300 (h) 920 (m)	NT
<b>23c</b>	H	H		360 (h) 170 (m)	-9% (10mg/kg)
<b>23d</b>	H	H		3100 (h) 7300 (m)	NT
<b>23e</b>	H	H		630 (h) 830 (m)	NT
<b>23f</b>	H	H		52 (h) 45 (m)	2% (3mg/kg)
<b>23g</b>	H	Et		860 (h) 210 (m)	NT
<b>23h</b>	H	Et		410 (h) 90 (m)	NT
<b>23i</b>	H	Et		290 (h) 110 (m)	NT
<b>23j</b>	H	Et		100 (h) 73 (m)	-100% (1 mg/kg) -73% (0.3 mg/kg)
<b>23k</b>	H	Et		640 (h) 310 (m)	NT
<b>23l</b>	Et	Me		110 (h) 50 (m)	-92% (3 mg/kg)
<b>23m</b>	Et	$\alpha$ -Me		85 (h) 53 (m)	-46% (3 mg/kg)
<b>23n</b>	Et	$\beta$ -Me		64 (h) 44 (m)	-93% (3 mg/kg)

<sup>a</sup>Assay values are the average of at least two independent determinations. <sup>b</sup>Enzyme species indicated between parentheses: *h* = human, *m* = mouse.

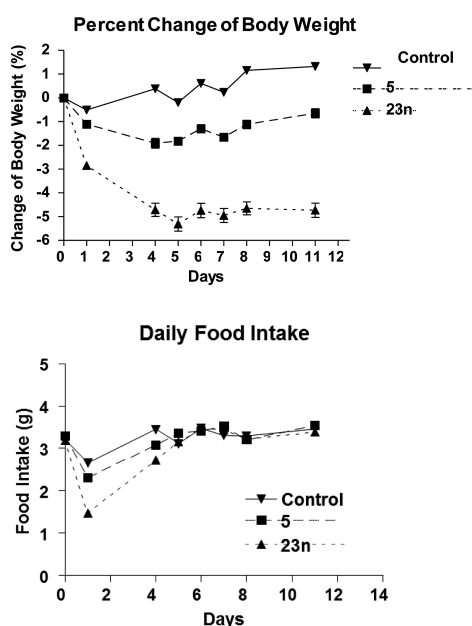
chronic efficacy study, benzooxazine **23n** demonstrated a statistically significant decrease in body weight (>5% for 30 mg/kg, PO, qd). In comparison, compound **5** induced a 2%



Table 4. Pharmacokinetic Parameters for Lead Compound 23n in Rats, Mice, Dogs, and Monkeys<sup>a</sup>

	PPTG 3 mg/kg (time point)	AUC ( $\mu\text{M}\cdot\text{h}$ ) <sup>b</sup>	Cl ( $\mu\text{L}/\text{min}/\text{Mcells}$ )	$C_{\text{max}}$ ( $\mu\text{M}$ )	$t_{1/2}$ (h)	F (%)
rat		41	10	9.1	3.0	75
mouse	−93% (2 h), −87% (12 h)	3.7	6.2	0.6	6.2	89
dog		23	16	3.3	3.0	
monkey		64	14	5.7	3.0	

<sup>a</sup>Assay values are the average of at least two independent determinations: 10 mg/kg for PO in rats, 1 mg/kg for PO in mice, 2 mg/kg for PO in dogs, and 3 mg/kg for PO in monkeys. <sup>b</sup>All values are mean values  $\pm$  SEM for  $n = 8$  ( $p < 0.01$ ).



**Figure 3.** Body weight change and food effects on DIO mice (dosed in 0.5% methylcellulose (vehicle) at 10 mg/kg/day for compound 5; in 0.5% methylcellulose suspension at 30 mg/kg/day for compound 23n) over a two-week period. Weight changes are registered as the percent to day-zero value from the same group of mice for each measurement time point. Food intake changes are expressed as the number of grams difference of food consumed to day-zero value from the same group of mice for each measurement time point.

body weight reduction after 10 mg/kg PO dosing. Interestingly, a transient drop in food intake (days 1–4) was observed for mice treated with lead compound 23n. No measurable differences in locomotive activity were observed in the drug-treated mice throughout the whole study, indicating that treatment did not cause any adverse behavior effect. This body weight reduction might be partly due to the reduced food intake. The exact mechanism of how selective DGAT1 inhibitors can affect food intake is not clear. It is hypothesized that inhibiting DGAT1 can affect fatty acid composition, distribution, and sensing mechanisms, which might exhibit a feedback mechanism on food intake.<sup>21</sup>

Compound 23n was also sent to a screening panel of 110 enzymes, receptors, and ion channels to further assess selectivity (data in Supporting Information). The results showed compound 23n had a clean off target profile ( $\text{IC}_{50} >$

10  $\mu\text{M}$ ) for 105 out of 110 targets in the panel, including potential targets that can affect food intake and body weight, such as the cannabinoid (CB1), cholecystokinin (CCK), dopamine (D2), histamine, serotonin, neuropeptide Y, and purinergic receptor (PX). The five targets from the panel that showed measurable inhibition with compound 23n are the peptidase CASP8 ( $\text{IC}_{50}$  6.8  $\mu\text{M}$ ), CASP9 ( $\text{IC}_{50}$  5.0  $\mu\text{M}$ ), EGF Receptor ( $\text{IC}_{50}$  7.5  $\mu\text{M}$ ), insulin receptor ( $\text{IC}_{50}$  5.7  $\mu\text{M}$ ), and prostanoid IP ( $\text{IC}_{50}$  1.0  $\mu\text{M}$ ). These off target activities are highly unlikely to be related to the food intake effect observed with compound 23n.

In summary, a novel class of benzomorpholine compounds has been identified as potent DGAT1 inhibitors, based on pharmacophore modeling. SAR investigations have led to the identification of several compounds with good pharmacokinetic and pharmaceutical profiles. *In vivo* mouse PPTG studies have shown that low doses of the DGAT1 inhibitors significantly reduce TG absorption and plasma levels following a lipid challenge. Treatment of DIO mice with the benzomorpholine lead 23n for 11 days showed inhibition of body weight gain and decrease in food intake. These results provide further insights into the use of DGAT1 inhibition as a novel approach for the treatment of metabolic diseases.

## ■ ASSOCIATED CONTENT

### 📄 Supporting Information

Experimental data details of syntheses and characterization, *in vitro* and *in vivo* biological assay for 8–23n. This material is available free of charge via the Internet at <http://pubs.acs.org>.

## ■ AUTHOR INFORMATION

### Corresponding Author

\*Phone: 732-594-2487. E-mail: [gang.zhou@merck.com](mailto:gang.zhou@merck.com).

### Notes

The authors declare no competing financial interest.

## ■ ACKNOWLEDGMENTS

We thank Dr. Malcolm MacCoss for suggestions; Dr. Grant Wishart for structure modeling; Tze-Ming Chan for NMR structure analysis; and Kung-I Feng for plasma stability assays.

## ■ ABBREVIATIONS

ACAT, acyl-CoA:cholesterol acyltransferase; CASP, caspase; CYP, cytochrome P; EGF, epidermal growth factor; hERG, human ether-à-gogo-related gene; ppg, p-glycoprotein; PPAR,

peroxisome proliferator activated receptor; PXR, Pregnane X receptor

## REFERENCES

- (1) Semenovich, C. F. Insulin resistance and atherosclerosis. *J. Clin. Invest.* **2006**, *116*, 1813–1822.
- (2) McGarry, J. D. Dysregulation of fatty acid metabolism in the etiology of type 2 diabetes. *Diabetes* **2002**, *51* (1), 7–18.
- (3) Shi, Y.; Burn, P. Lipid metabolic enzymes: emerging drug targets for treatment of obesity. *Nat. Rev.* **2004**, *3*, 695–710.
- (4) Zammit, V. A.; Buckett, L. K.; Turnbull, A. V.; Wure, J.; Proven, A. Diacylglycerol acyltransferases: Potential roles as pharmacological targets. *Pharmacol. Ther.* **2008**, *118*, 295–302.
- (5) Yen, C. E.; Stone, S. J.; Koliwad, D.; Harris, C.; Farese, R. V., Jr. DGAT enzymes and triacylglycerol biosynthesis. *J. Lipid Res.* **2008**, *49*, 2283–2301.
- (6) Chen, H. C.; Farese, R. V. DGAT and triglyceride synthesis: a new target for obesity treatment. *Trends Cardiovasc. Med.* **2000**, *10*, 188–192.
- (7) Cases, S.; Smith, S. J.; Zheng, Y-W; Myers, H. M.; Lear, S. R.; Sande, E.; Novak, S.; Collins, C.; Welch, C. B.; Lusis, A. J.; Erickson, S. K.; Farese, R. V., Jr. Identification of a gene encoding an acyl CoA:diacylglycerol acyltransferase, a key enzyme in triacylglycerol synthesis. *Proc. Natl. Acad. Sci. U.S.A.* **1998**, *95*, 13018–13023.
- (8) Cases, S.; Stone, S. J.; Zhou, P.; Yen, E.; Tow, B.; Voelker, T.; Farese, R. V., Jr. Cloning of DGAT2, a second mammalian diacylglycerol acyltransferase, and related family members. *J. Biol. Chem.* **2001**, *276*, 38870–38876.
- (9) Smith, S. J.; Cases, S.; Jensen, D. R.; Chen, H. C.; Sande, E.; Tow, B.; Sanan, D. A.; Raber, J.; Eckel, R. H.; Farese, R. V., Jr. Obesity resistance and multiple mechanisms of triglyceride synthesis in mice lacking DGAT. *Nat. Genet.* **2000**, *25*, 87–90.
- (10) Chen, H. C.; Jensen, D. R.; Myers, H. M.; Eckel, R. H.; Farese, R. V. Obesity resistance and enhanced glucose metabolism in mice transplanted with white adipose tissue lacking acyl CoA:diacylglycerol acyltransferase 1. *J. Clin. Invest.* **2003**, *111* (11), 1715–1722.
- (11) Chen, H. C.; Ladha, Z.; Smith, S. J.; Farese, R. V. Analysis of energy expenditure at different ambient temperatures in mice lacking DGAT1. *Am. J. Physiol. Endocrinol. Metab.* **2003**, *284* (1), 213–218.
- (12) Stone, S. J.; Myers, H. M.; Watkins, S. M.; Brown, B. E.; Feingold, K. R.; Elias, P. M.; Farese, R. V., Jr. Lipopenia and skin barrier abnormalities in DGAT2-deficient mice. *J. Biol. Chem.* **2004**, *279*, 11767–11776.
- (13) King, A. J.; Judd, A. S.; Souers, A. J. Inhibitors of diacylglycerol acyltransferase: a review of 2008 patents. *Expert Opin. Ther. Pat.* **2010**, *20*, 19–29.
- (14) Birch, A. M.; Bowker, S. S.; Butlin, R. J.; Donald, C. S.; McCoull, W.; Nowak, T.; Plowright, A. T. Oxadiazole derivatives as dgat inhibitors. Patent WO 2006/064189, 2006.
- (15) Fox, B. M.; Iio, K.; Li, K.; Choi, R.; Inaba, T.; Jackson, S.; Sagawa, S.; Shan, B.; Tanaka, M.; Yoshida, A.; Kayser, F. Discovery of pyrrolopyridazines as novel DGAT1 inhibitors. *Bioorg. Med. Chem. Lett.* **2010**, *20*, 6030–6033.
- (16) Devita, R. J.; Pinto, S. Current Status of the Research and Development of Diacylglycerol O-Acyltransferase 1 (DGAT1) Inhibitors. *J. Med. Chem.* **2013**, *56*, 9820–9825.
- (17) Smith, R.; Campbell, A.-M.; Coish, P.; Dai, M.; Jenkins, S.; Lowe, D.; O'Connor, S.; Su, N.; Wang, G.; Zhang, M.; Zhu, L. Preparation of Benzazolylaminobiphenyloxoalkanoates for the Treatment of Obesity. US 2004/0224997, 2004.
- (18) Zhao, G.; Souers, A. J.; Voorbach, M.; Falls, H. D.; Droz, B.; Brodjian, S.; Lau, Y. Y.; Iyengar, R. R.; Gao, J.; Judd, A. S.; Wagaw, S. H.; Ravn, M. M.; Engstrom, K. M.; Lynch, J. K.; Mulhern, M. M.; Freeman, J.; Dayton, B. D.; Wang, X.; Grihalde, N.; Fry, D.; Beno, D. W. A.; Marsh, K. C.; Su, Z.; Diaz, G. J.; Collins, C. A.; Sham, H.; Reilly, R. M.; Brune, M. E.; Kym, P. R. Validation of diacyl glycerolacyltransferase I as a novel target for the treatment of obesity and dyslipidemia using a potent and selective small molecule inhibitor. *J. Med. Chem.* **2008**, *51*, 380–383.
- (19) Birch, A. M.; Birtles, S.; Buckett, L. K.; Kemmitt, P. D.; Smith, G. J.; Smith, T. J. D.; Turnbull, A. V.; Wang, S. J. Y. Discovery of a potent, selective, and orally efficacious pyrimidinoxazinyl bicyclooctaneacetic acid diacylglycerol acyltransferase-1 inhibitor. *J. Med. Chem.* **2009**, *52*, 1558–1568.
- (20) Lee, B.; Fast, A. M.; Zhu, J.; Cheng, J.; Buhman, K. K. Intestine specific expression of acyl CoA:diacylglycerol acyltransferase I reverses resistance to diet-induced hepatic steatosis and obesity in DGAT1<sup>-/-</sup> mice. *J. Lipid Res.* **2010**, *51*, 1770–1780.
- (21) Okawa, M.; Fujii, K.; Ohbuchi, K.; Okumoto, M.; Aragane, K.; Sato, H.; Tamai, Y.; Seo, T.; Itoh, Y.; Yoshimoto, R. Role of MGAT2 and DGAT1 in the release of gut peptides after triglyceride ingestion. *Biochem. Biophys. Res. Commun.* **2009**, *390*, 377–381.